Production of Laser in a Quasi-Three-Level System: An Experimental Approach*

Balogun Bashiru Bolaji – 201507796

Department of Physics and Astronomy,
Faculty of Sciences,
University of Porto.
Rua do Campo Alegre 687, 4169-007 Porto, Portugal

* This experimental demonstration was done on the 4th of April, 2016 at FCUP.

Abstract

As optical amplifiers and laser sources represent very important optical devices in numerous applications ranging from telecommunications to medicine, the production of laser in a quasi-three-level system becomes sine qua non. A quasi-three-level laser medium (such as erbium-doped fiber) is one with a kind of intermediate situation, where the lower laser level is so close to the ground state that an appreciable population in that level occurs in thermal equilibrium at the operating temperature. Hence, this paper presents a detailed operational study of the erbium-doped fiber amplifier (EDFA) for the production of laser based on a Fabry-Perot cavity built with two fiber Bragg gratings (FBG) with a small mismatch in the Bragg wavelength. In a broader sense, optical amplifiers are the basis of all lasers. With a simple extension to the basic amplifier kits, an erbium doped fiber ring laser was constructed and characterized. The power characteristics (threshold and slope efficiency) as a function of output coupling ratio were vividly studied. Finally, observations and precautions made during the experiment were presented alongside with the improvement of the functioning of the experimental setup.

1.0 Introduction

Direct optical amplification using erbium doped fiber amplifiers (EDFAs) is now preferred over optoelectronic repeaters as the primary means of restoring the signal power in long distance fiber optic links and branched networks. These amplifiers naturally provide gain at very high bit rates and at many wavelengths in a broad band stretching from 1530 *nm* to 1580 *nm*. Without them, high data rate wavelength division multiplexed communication system would not exist. They also enable the implementation of multi-branch optical networks by very conveniently overcoming the large splitting losses of a high order multi-layer system. In addition, lasers (essentially optical oscillators) are simply optical amplifiers with positive feedback, again highlighting the importance of optical amplifiers in modern photonics systems. Engineering and science students therefore benefit from a good understanding and practical working knowledge of optical amplifiers and lasers. Here we report the design, hardware, experimental procedures and results of student laboratory kit which enable the experimental investigation of erbium doped fiber amplifiers and ring lasers.

The specific objectives of the EDF optical amplifiers and lasers experiment are to enable students to experimentally investigate the principles and characteristics of erbium doped fiber amplifiers and lasers. The underlying aims are to allow students gain practical, hands experience of EDFA and lasers in particular and to consolidate their conceptual understanding and knowledge of optical amplifiers and lasers in general. To achieve the above aims and objectives the experimental investigation was generally defined as follows;

- Understand the principle of operation of the erbium-doped fiber amplifier (EDFA).
- Construct an EDFA and an erbium-doped fiber laser.
- Measure and calculate the essential parameters of the constructed EDFA.

The approach employed in the experiment of fiber laser is based on a Fabry-Perot cavity built with two fiber Bragg gratings (FBG) with a small mismatch in the Bragg wavelength. Noteworthy, the laser is achieved when this mismatch is reduced through longitudinal stress applied to one of the gratings. By this, the sensitivity to the laser characteristics is dependent on the cavity parameters (i.e. mirror reflectivity) which is consequently related to the threshold and slope efficiency. In general, FBGs are used as guided optical sensors transversally. Typically, in this report, optical sensing structures such as FBGs are used in an inverse way to control the laser cavity parameters.

2.0 Theoretical Background

2.1 Fiber Bragg Grating

A fiber Bragg grating (FBG) is a type of distributed Bragg reflector constructed in a short segment of optical fiber that reflects particular wavelengths of light and transmits all others. This is achieved by creating a periodic variation in the refractive index of the fiber core, which generates a wavelength-specific dielectric mirror. A fiber Bragg grating can therefore be used as an inline optical filter to block certain wavelengths, or as a wavelength-specific reflector. FBG is basically a periodic perturbation of refractive index along the waveguide formed by exposing it to an intense ultraviolet periodic light (such as UV laser) pattern created by the interference of two light beams at the same wavelength. Figure 1 shows a FBG structure with refractive index profile and spectral response.

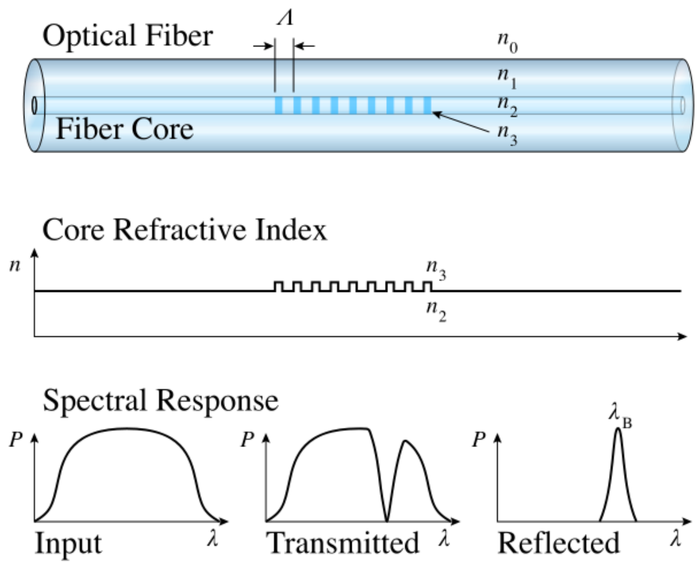

Figure 1: A Fiber Bragg Grating structure, with refractive index profile and spectral response

There are basically two methods widely used for the fabrication of FBGs, these are: interference and masking. The method that is preferable depends on the type of grating to be manufactured. Normally a germanium-doped silica fiber is used in the manufacture of fiber Bragg gratings. The germanium-doped fiber is photosensitive, which means that the refractive index of the core changes with exposure to UV light. Hence, permanent change of the refractive index is achieved through UV exposure. The amount of the change depends on the intensity and duration of the exposure as well as the photosensitivity of the fiber. To write a high reflectivity fiber Bragg grating directly in the fiber the level of doping with germanium needs to be high. However, standard fibers can be used if the photosensitivity is enhanced by pre-soaking the fiber in hydrogen. More recently, fiber Bragg gratings have also been written in polymer fibers.

Usually, the refractive index perturbation consists of a core geometry variation and a core index perturbation, both inducing an effective index perturbation. The resulting uniform sinusoidal Bragg index grating along the core of the waveguide can be expressed as;

$$n(\varrho) = n_0 + \Delta n \cos\left(\frac{2\pi\varrho}{\Lambda}\right) \qquad (1)$$

Where n_0 is the average index, Δn is the UV induced refractive index perturbation, ϱ is the distance along the longitudinal axis and Λ is the spatial period of the index modulation. For this periodic modulation, the reflected wavelength also called Bragg wavelength is then given as;

$$\lambda_B = 2n_e\Lambda \qquad (2)$$

Where n_e is the effective index of the propagating mode. Therefore, the Bragg wavelength can be changed by varying the period, such as stretching or compressing the fiber or by affecting the modal effective index such as by temperature change.

FBGs have been used in myriads of application in recent time. These are; sensor, communication, process match of active and massive fivers and in the production of fiber lasers among others. However, their usage in FBGs have greatly received keen attention by researchers across the globe. The development of high power fiber lasers has generated a new set of applications for fiber Bragg gratings, operating at power levels that were previously thought impossible. In the case of a simple fiber laser, the FBG's can be used as the high reflector (HR) and output coupler (OC) to form the laser cavity. The gain for the laser is provided by a length of rare earth doped optical fiber, with the most common form using Yb^{3+} ions as the active lasing ion in the silica fiber. These Yb-doped fiber lasers first operated at the 1 kW CW power level in 2004 based on free space cavities but were not shown to operate with fiber Bragg grating cavities until much later.

Such monolithic, all-fiber devices are produced by many companies worldwide and at power levels exceeding 1 *kW*. The major advantage of these all fiber systems, where the free space mirrors are replaced with a pair of fiber Bragg gratings (FBG's), is the elimination of realignment during the life of the system, since the FBG is spliced directly to the doped fiber and never needs adjusting. The challenge is to operate these monolithic cavities at the *kW* CW power level in large mode area (LMA) fibers such as 20/400 (20 *um* diameter core and 400 *um* diameter inner cladding) without premature failures at the intra-cavity splice points and the gratings. Once optimized, these monolithic cavities do not need realignment during the life of the device, removing any cleaning and degradation of fiber surface from the maintenance schedule of the laser.

However, the packaging and optimization of the splices and FBGs themselves are non-trivial at these power levels as are the matching of the various fibers, since the composition of the Yb-doped fiber and various passive and photosensitive fibers needs to be carefully matched across the entire fiber laser chain. Although the power handling capability of the fiber itself far exceeds this level, and is possibly as high as >30 kW CW, the practical limit is much lower due to component reliability and splice losses.

2.2 Population Inversion

In science, specifically statistical mechanics, a population inversion occurs while a system (such as a group of atoms or molecules) exists in a state with more members in an excited state than in lower energy states. It is called an "inversion" because in many familiar and commonly encountered physical systems, this is not possible. The concept is of fundamental importance in laser science because the production of a population inversion is a necessary step in the workings of a standard laser. To understand the concept of a population inversion, it is necessary to understand some thermodynamics and the way that light interacts with matter. To do so, it is useful to consider a very simple assembly of atoms forming a laser medium. Assume there are a group of N atoms, each of which is capable of being in one of two energy states: either

i. The ground state, with energy E_1; or
ii. The excited state with energy E_2, with $E_2 > E_1$.

Hence, the number of these atoms which are in the ground state is given by N_1, and the number in the excited state N_2. Since there are N atoms in total,

$$N_2 + N_2 = N$$

The energy difference between the two states, given by $\Delta E_{12} = E_2 - E_1$, determines the characteristic frequency υ_{12} of light which will interact the atoms; this is given by the relation

$$E_2 - E_1 = \Delta E = h\upsilon_{12}$$

h being the plank's constant. If the group of atoms is in thermal equilibrium, it can be shown from Maxwell–Boltzmann statistics that the ratio of the number of atoms in each state is given by the ratio of two Boltzmann distributions, the Boltzmann factor:

$$\frac{N_2}{N_1} = \exp\frac{-(E_2 - E_1)}{kT}$$

where T is the thermodynamic temperature of the group of atoms, and k is Boltzmann's constant.

Alternatively, the populations of the two states at room temperature ($T \approx 300$ K) for an energy difference ΔE that corresponds to light of a frequency corresponding to visible light ($\nu \approx 5\times10^{14}$ Hz). In this case $\Delta E = E_2 - E_1 \approx 2.07$ eV, and $kT \approx 0.026\ eV$. Since $E_2 - E_1 \gg kT$, it follows that the argument of the exponential in the equation above is a large negative number, and as such N_2/N_1 is vanishingly small; i.e., there are almost no atoms in the excited state. When in thermal equilibrium, then, it is seen that the lower energy state is more populated than the higher energy state, and this is the normal state of the system. As T increases, the number of electrons in the high-energy state (N_2) increases, but N_2 never exceeds N_1 for a system at thermal equilibrium; rather, at infinite temperature, the populations N_2 and N_1 become equal. In other words, a population inversion ($N_2/N_1 > 1$) can never exist for a system at thermal equilibrium. To achieve population inversion therefore requires pushing the system into a non-equilibrated state.

2.3 Interaction of light with matter

Majorly, the interaction of light with matter have led to plethoric amount of processes which are aiding the modern-day technologies. There are three types of possible interactions between a system of atoms and light. These are;

Absorption: If light (photons) of frequency υ_{12} passes through the group of atoms, there is a possibility of the light being absorbed by atoms which are in the ground state, which will cause them to be excited to the higher energy state. The rate of absorption is proportional to the radiation intensity of the light, and also to the number of atoms currently in the ground state, N_1.

Spontaneous Emission: If atoms are in the excited state, spontaneous decay events to the ground state will occur at a rate proportional to N_2, the number of atoms in the excited state. The energy difference between the two states ΔE_{21} is emitted from the atom as a photon of frequency υ_{21} as given by the frequency-energy relation above. The photons are emitted stochastically, and there is no fixed phase relationship between photons emitted from a group of excited atoms; in other words, spontaneous emission is incoherent. In the absence of other processes, the number of atoms in the excited state at time t, is given by;

$$N_2(t) = N_2(0)\exp\frac{-t}{\tau_{21}}$$

Where $N_2(0)$ is the number of excited atoms at time $t = 0$, and τ_{21} is the mean lifetime of the transition between the two states.

Stimulated Emission: If an atom is already in the excited state, it may be perturbed by the passage of a photon that has a frequency υ_{21} corresponding to the energy gap ΔE of the excited state to ground state transition. In this case, the excited atom relaxes to the ground state, and it produces a second photon of frequency υ_{21}. The original photon is not absorbed by the atom, and so the result is two photons of the same frequency. This process is known as *stimulated emission*.

Specifically, an excited atom will act like a small electric dipole which will oscillate with the external field provided. One of the consequences of this oscillation is that it encourages electrons to decay to the lowest energy state. When this happens due to the presence of the electromagnetic field from a photon, a photon is released in the same phase and direction as the "stimulating" photon, and is called stimulated emission. Figure 2 illustrates this concept better;

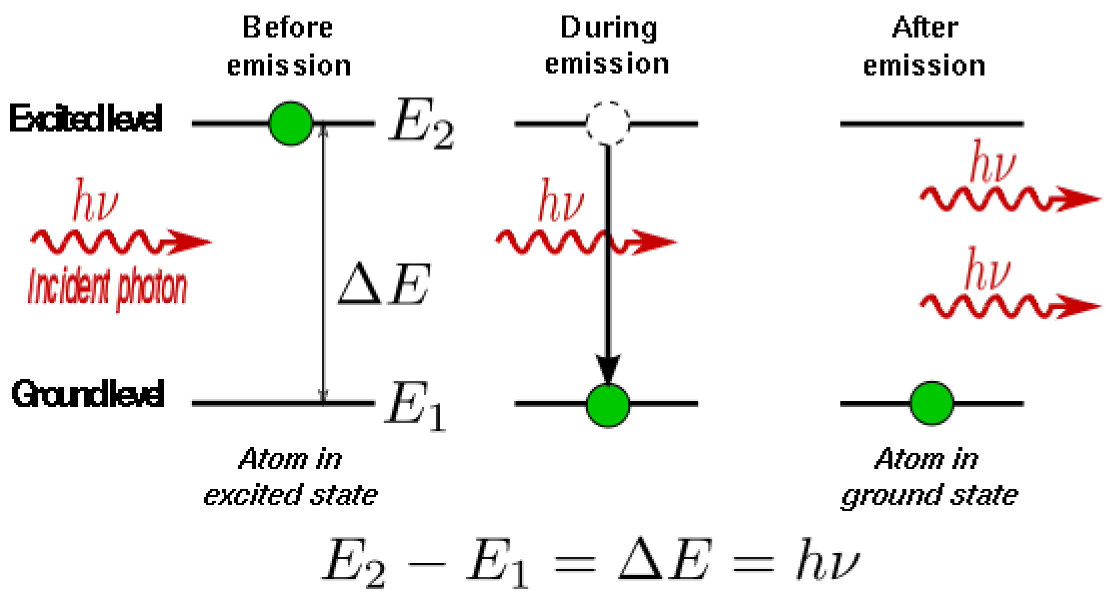

Figure 2: Schematic illustration of stimulated emission

The rate at which stimulated emission occurs is proportional to the number of atoms N_2 in the excited state, and the radiation density of the light. The base probability of a photon causing stimulated emission in a single excited atom was shown by Albert Einstein to be exactly equal to the probability of a photon being absorbed by an atom in the ground state. Therefore, when the numbers of atoms in the ground and excited states are equal, the rate of stimulated emission is equal to the rate of absorption for a given radiation density.

The critical detail of stimulated emission is that the induced photon has the same frequency and phase as the incident photon. In other words, the two photons are coherent. It is this property that allows optical amplification, and the production of a laser system. During the operation of a laser, all three light-matter interactions described above are taking place. Initially, atoms are energized from the ground state to the excited state by a process called *pumping*, described below. Some of these atoms decay via spontaneous emission, releasing incoherent light as photons of frequency, υ_{21} . These photons are fed back into the laser medium, usually by an optical resonator. Some of these photons are absorbed by the atoms in the ground state, and the photons are lost to the laser process. However, some photons cause stimulated emission in excited-state atoms, releasing another coherent photon. In effect, this results in *optical amplification*.

If the number of photons being amplified per unit time is greater than the number of photons being absorbed, then the net result is a continuously increasing number of photons being produced; the laser medium is said to have a gain of greater than unity.

Recall from the descriptions of absorption and stimulated emission above that the rates of these two processes are proportional to the number of atoms in the ground and excited states, N_1 and N_2, respectively. If the ground state has a higher population than the excited state ($N_1 > N_2$), then the absorption process dominates, and there is a net attenuation of photons. If the populations of the two states are the same ($N_1 = N_2$), the rate of absorption of light exactly balances the rate of emission; the medium is then said to be *optically transparent*.

If the higher energy state has a greater population than the lower energy state ($N_1 < N_2$), then the emission process dominates, and light in the system undergoes a net increase in intensity. It is thus clear that to produce a faster rate of stimulated emissions than absorptions, it is required that the ratio of the populations of the two states is such that $N_2/N_1 > 1$; In other words, a population inversion is required for laser operation.

2.4 Creating a Population Inversion

As described above, a population inversion is required for laser operation, but cannot be achieved in our theoretical group of atoms with two energy-levels when they are in thermal equilibrium. In fact, any method by which the atoms are directly and continuously excited from the ground state to the excited state (such as optical absorption) will eventually reach equilibrium with the de-exciting processes of spontaneous and stimulated emission. At best, an equal population of the two states, $N_1 = N_2 = N/2$, can be achieved, resulting in optical transparency but no net optical gain.

2.4.1 Three-level Lasers

To achieve non-equilibrium conditions, an indirect method of populating the excited state must be used. To understand how this is done, we may use a slightly more realistic model, that of a *three-level laser*. Again consider a group of N atoms, this time with each atom able to exist in any of three energy states, levels 1, 2 and 3, with energies E_1, E_2, and E_3, and populations N_1, N_2, and N_3, respectively. Assume that $E_1 < E_2 < E_3$; that is, the energy of level 2 lies between that of the ground state and level 3.

Initially, the system of atoms is at thermal equilibrium, and the majority of the atoms will be in the ground state, i.e., $N_1 \approx N$, $N_2 \approx N_3 \approx 0$. If we now subject the atoms to light of a frequency $\upsilon_{13} = \frac{1}{h}(E_3 - E_1)$, the process of optical absorption will excite the atoms from the ground state to level 3. This process is called *pumping*, and does not necessarily always directly involve light absorption; other methods of exciting the laser medium, such as electrical discharge or chemical reactions, may be used. The level 3 is sometimes referred to as the *pump level* or *pump band*, and the energy transition $E_1 \rightarrow E_3$ as the *pump transition*, which is shown as the arrow marked **P** in the Figure 3.

If we continuously pump the atoms, we will excite an appreciable number of them into level 3, such that $N_3 > 0$. To have a medium suitable for laser operation, it is necessary that these excited atoms quickly decay to level 2. The energy released in this transition may be emitted as a photon (spontaneous emission), however in practice the 3→2 transition (labeled **R** in the diagram) is usually *radiationless*, with the energy being transferred to vibrational motion (heat) of the host material surrounding the atoms, without the generation of a photon.

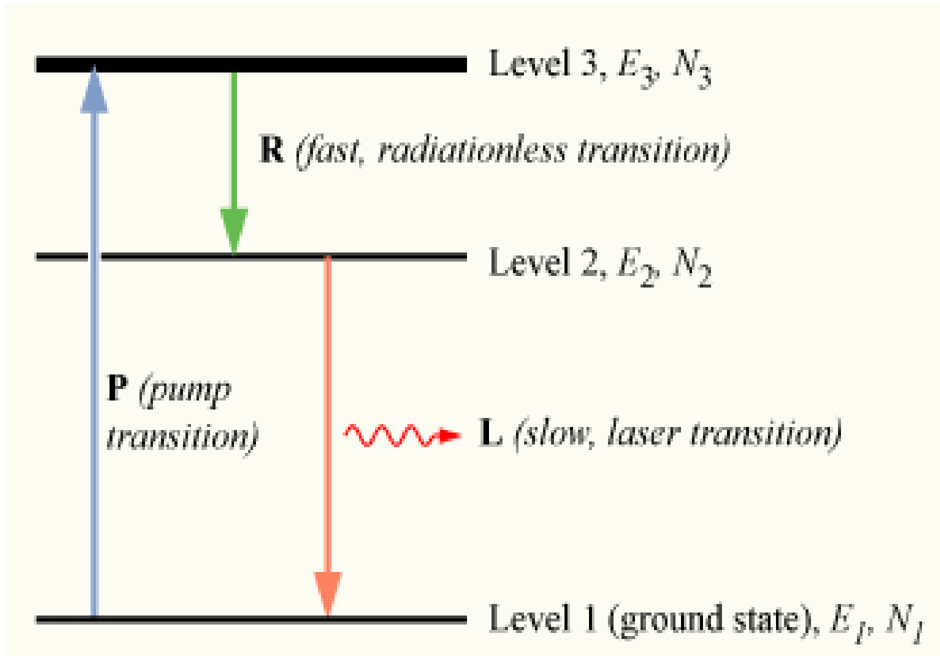

Figure 4: A three-level laser energy diagram

An atom in level 2 may decay by spontaneous emission to the ground state, releasing a photon of frequency υ_{12} (given by $E_2 - E_1 = h\upsilon_{21}$), which is shown as the transition **L**, called the *laser transition* in the diagram. If the lifetime of this transition, τ_{21} is much longer than the lifetime of the radiationless 3 → 2 transition τ_{32} (if $\tau_{21} \gg \tau_{32}$, known as a *favourable lifetime ratio*), the population of the E_3 will be essentially zero ($N_3 \approx 0$) and a population of excited state atoms will accumulate in level 2 ($N_2 > 0$). If over half the N atoms can be accumulated in this state, this will exceed the population of the ground state N_1. A population inversion ($N_2 > N_1$) has thus been achieved between level 1 and 2, and optical amplification at the frequency υ_{21} can be obtained.

Because at least half the population of atoms must be excited from the ground state to obtain a population inversion, the laser medium must be very strongly pumped. This makes three-level lasers rather inefficient, despite being the first type of laser to be discovered (based on a ruby laser medium, by Theodore Maiman in 1960). A three-level system could also have a radiative transition between level 3 and 2, and a non-radiative transition between 2 and 1. In this case, the pumping requirements are weaker. An example of a three-level laser medium is ruby ($Cr^{3+}:Al_2O_3$), as used by Maiman for the first laser.

2.4.2 Four-level Lasers

Here, there are four energy levels, energies E_1, E_2, E_3, E_4, and populations N_1, N_2, N_3, N_4, respectively. The energies of each level are such that$E_1 < E_2 < E_3 < E_4$. In this system, the pumping transition **P** excites the atoms in the ground state (level 1) into the pump band (level 4). From level 4, the atoms again decay by a fast, non-radiative transition **Ra** into the level 3. Since the lifetime of the laser transition **L** is long compared to that of **Ra** ($\tau_{32} \gg \tau_{43}$), a population accumulates in level 3 (the *upper laser level*), which may relax by spontaneous or stimulated emission into level 2 (the *lower laser level*). This level likewise has a fast, non-radiative decay **Rb** into the ground state.

As before, the presence of a fast, radiationless decay transition results in the population of the pump band being quickly depleted ($N_4 \approx 0$). In a four-level system, any atom in the lower laser level E_2 is also quickly de-excited, leading to a negligible population in that state ($N_2 \approx 0$). This is important, since any appreciable population accumulating in level 3, the upper laser level, will form a population inversion with respect to level 2. That is, as long as $N_3 > 0$, then $N_3 > N_2$, and a population inversion is achieved. Thus optical amplification, and laser operation, can take place at a frequency of ($E_3 – E_2 = h$).

Since only a few atoms must be excited into the upper laser level to form a population inversion, a four-level laser is much more efficient than a three-level one, and most practical lasers are of this type. In reality, many more than four energy levels may be involved in the laser process, with complex excitation and relaxation processes involved between these levels. In particular, the pump band may consist of several distinct energy levels, or a continuum of levels, which allow optical pumping of the medium over a wide range of wavelengths.

Note that in both three- and four-level lasers, the energy of the pumping transition is greater than that of the laser transition. This means that, if the laser is optically pumped, the frequency of the pumping light must be greater than that of the resulting laser light. In other words, the pump wavelength is shorter than the laser wavelength. It is possible in some media to use multiple photon absorptions between multiple lower-energy transitions to reach the pump level; such lasers are called *up-conversion* lasers.

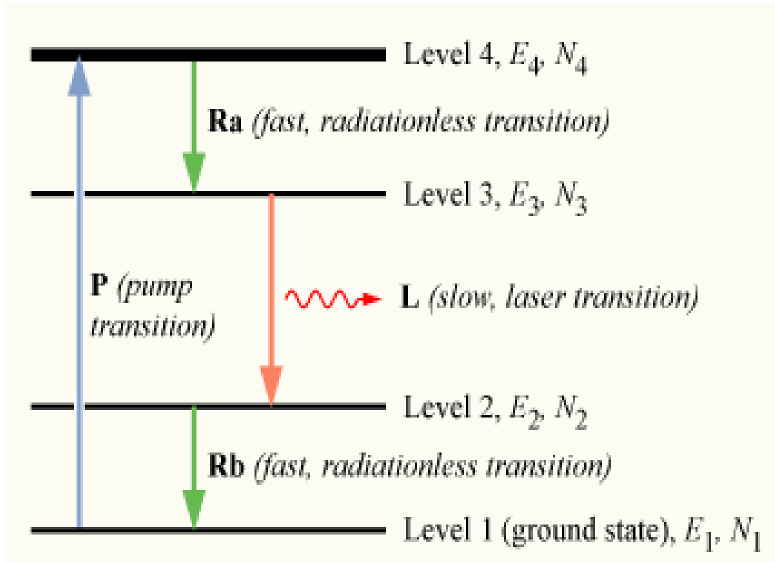

Figure 4: A three-level laser energy diagram

While in many lasers the laser process involves the transition of atoms between different electronic energy states, as described in the model above, this is not the only mechanism that can result in laser action. For example, there are many common lasers (e.g., dye lasers, carbon dioxide lasers) where the laser medium consists of complete molecules, and energy states correspond to vibrational and rotational modes of oscillation of the molecules. This is the case with water masers, that occur in nature. In some media it is possible, by imposing an additional optical or microwave field, to use quantum coherence effects to reduce the likelihood of an excited-state to ground-state transition. This technique, known as lasing without inversion, allows optical amplification to take place without producing a population inversion between the two states.

2.4.3 Quasi-Three-Level Systems

A quasi-three-level laser medium is one with a kind of intermediate situation, where the lower laser level is so close to the ground state that an appreciable population in that level occurs in thermal equilibrium at the operating temperature. As a consequence, the unpumped gain medium causes some reabsorption loss at the laser wavelength, and transparency is reached only for some finite pump intensity. For higher pump intensities, there is gain, as required for laser operation.

Examples of quasi-three-level media are all ytterbium-doped gain media (e.g. Yb:YAG, or Yb:glass as used in optical fibers), neodymium-doped media operated on the ground state transition (e.g. 946 nm for Nd:YAG), thulium-doped crystals and glasses for 2-µm emission, and erbium-doped media for 1.5 or 1.6-µm emission, such as erbium-doped fiber amplifiers which is particularly considered in this experiment.

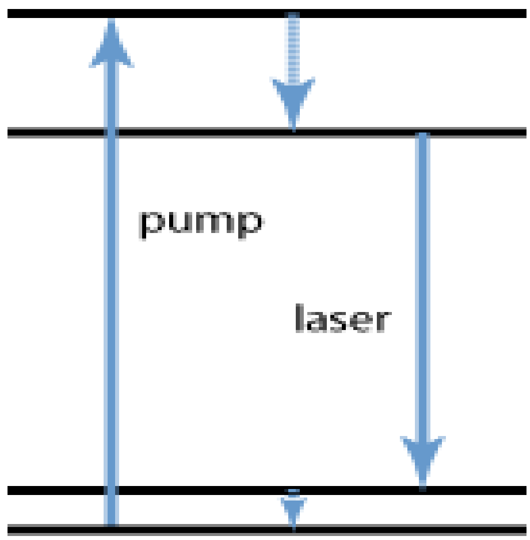

Figure 5: A Quasi-three-level laser energy diagram

An important fact is that the spectral shape of the optical gain in a quasi-three-level laser medium depends on the excitation level, because this affects the balance between emission and reabsorption. As a consequence, the laser wavelength obtained may depend on the resonator losses: high losses require a higher gain, and thus a higher excitation level, and consequently a shorter wavelength of maximum gain. (Note that the reabsorption is stronger at shorter wavelengths, thus particularly reducing the short-wavelength net gain for low excitation levels.) Similarly, the wavelength of maximum gain can be reduced by reducing the doping concentration, because this also implies a higher excitation density. On the other hand, this measure may reduce the efficiency of pump absorption. Therefore, there can be a trade-off between short-wavelength operation (with small quantum defect) and efficient pump absorption.

There can actually be a smooth transition from three-level to four-level gain characteristics with increasing laser wavelength. For example, erbium-doped glass always shows strong three-level behavior around 1535 nm but nearly four-level behavior for long wavelengths of e.g.

1600 nm. Similarly, ytterbium-doped glass exhibits pronounced three-level characteristics for wavelengths below ≈ 1040 nm, and the same holds for Yb:YAG lasers at 1030 nm and for lasers based on many other rare earth crystals. For operation at such wavelengths, a large inversion density is required for overcoming the reabsorption loss. For longer wavelengths, as sometimes used particularly in fiber lasers, there is hardly any reabsorption, and in a long fiber only a very low excitation density may be required to obtain sufficient gain.

Pronounced three-level behavior is inevitable for gain media with a very small quantum defect, because this enforces a small energy spacing between the lower laser level and the ground state, so that thermal population of the lower laser level is significant. By reducing the temperature of the laser crystal, it is possible to obtain less pronounced three-level characteristics, i.e., a reduced degree of reabsorption on the laser wavelength. This is essentially because the population in higher-lying sublevels of the ground state manifold is reduced. As an example, Yb:YAG has pronounced three-level characteristics at 1030 nm when operated at room temperature, while essentially four-level characteristics are obtained for cryogenic operation at 77 K (the temperature of liquid nitrogen). Note that the gain media of semiconductor lasers actually also behave like three-level lasers, exhibiting losses in the unpumped state and a shape of the gain spectrum which depends on the excitation density.

2.5 Theoretical Consideration of Erbium Doped Fiber Laser and Pumping Scheme

Erbium doped fiber laser is generally characterized by a pump laser threshold (P_{th}) given as:

$$P_{th} = \frac{\gamma + \sigma_a N_t \ell}{\eta_p} \left(\frac{h v_p}{\tau}\right) \left(\frac{A}{\sigma_e + \sigma_a}\right)$$

where, h is the Plank's constant, σ_a and σ_e are respectively the absorption and emission cross-section, N_t is the number of active atoms per unit volume, ℓ is the length of the active medium, η_p is the pump laser efficiency, v_p is the frequency of the pump laser, τ is the upper level lifetime, A is the section of the active medium and γ is the single pass logarithmic loss.

However, the total logarithmic loss per pass arises from the intrinsic loss (γ_i) and from the losses induced by the two reflecting mirrors i.e. $\gamma_1 = -\ln(R_i)$ and $\gamma_2 = -\ln(R_i)$, and it is given as;

$$\gamma = \gamma_i + \frac{\gamma_1 + \gamma_2}{2}$$

Assuming that both gratings are identical in reflectivity, with central Gaussian profile,

$$R_i(\lambda) = R_0 \exp\left(-\frac{(\lambda - \lambda_2)^2}{\omega_\lambda^2}\right),$$

where R_0 is the maximum reflectivity and ω_λ is the $1/\mathrm{e}$ half width, we get

$$\gamma_1 = -1 \ln R_0 + \frac{(\lambda - \lambda_1)^2}{\omega_\lambda^2}$$

And

$$\gamma_2 = -1 \ln R_0 + \frac{(\lambda - \lambda_2)^2}{\omega_\lambda^2}$$

As laser emission occurs at the wavelength where losses are minimum, it can be easily shown that the laser emission will take place at $\lambda_L = (\lambda_1/\lambda_2)/2$ if both gratings overlap. As $(\lambda_L - \lambda_1)^2 = (\lambda_L - \lambda_2)^2$. Using equations above, we have the pump laser threshold (P_{th}) given as follows;

$$P_{th} = \left(2\gamma_i - \ln R_0 + \sigma_a N_t \ell + \frac{(\lambda - \lambda_2)^2}{\omega_\lambda^2} + \right)\left(\frac{h v_p A}{\eta_p \tau (\sigma_e + \sigma_a)}\right) = K\left(Q + \frac{(\lambda - \lambda_2)^2}{\omega_\lambda^2}\right)$$

This confirms the quadratic behaviour of the laser threshold pump power with grating shift.

The laser efficiency (η_s), defined as a slope of the laser output power versus pump power, above the threshold, is given as;

$$\eta_s = \eta_p \left(\frac{h v_L A_b}{h v_p A}\right)\left(\frac{\gamma_2}{2\gamma}\right)$$

Where v_L is the laser emission frequency and A_b is the laser mode area inside the fiber. The threshold can further be re-written as;

$$\frac{1}{\eta_s} = \frac{2 v_p A}{\eta_p v_\ell A_b}\left(\frac{\gamma_i}{\gamma_i} + 1\right) = \frac{2 v_p A}{\eta_p v_\ell A_b}\left(\frac{\gamma_i}{-\ln R_0 + \frac{(\lambda - \lambda_2)^2}{\omega_\lambda^2}} + 1\right)$$

Hence using this equation with knowledge of maximum reflectivity and FWHM of the gaussian profile of the laser characteristics; intrinsic loss (γ_i) and the laser pump efficiency (η_p) can estimation be estimated.

3.0 Experimental Setup

The setup employed in this experiment is shown in figure 6. The optical pumping including optical isolator for the laser diode used as source is modelled ADC Telecommunications 978B200 – see figure 6. The output of the optical pump is fed directly into the optical cavity as shown in Figure 7. The Two similar fiber Bragg gratings (FBGs) in which the erbium doped fiber (EDF – 200cm long) is attached in between is fed into a wavelength division multiplexer (WDM) modelled EPT SMWDM980/1550. The WDM is to unsure separation of the wavelength separation. As the FBG is sensitive to both temperature and strain, we made use of the later while neglecting the former. Hence, the first FBG serving as the input mirror is mounted on a micromechanical translation stage for cavity detuning – see figure 8. The fiber is glued to the stage frame and to the moving block which allows for the stretching of the FBG 1 positioned between 100mm apart. The second FBG serving as the output mirror at the end of the cavity is fed into the WDM which separates the laser emission from the FBG2. The FBG2 attached to the WDM serves either an optical spectrum analyzer (OSA, Ando AQ-6315B) or an optical power detector (EXFO IQ-203).

Figure 6: Picture of the laser diode used as source to achieve optical pumping of the system

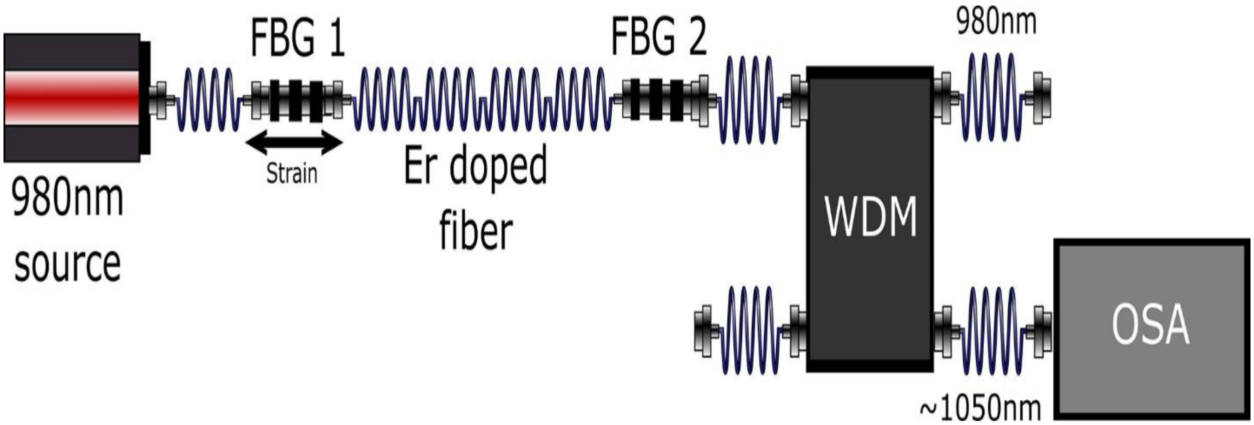

Figure 7: Experimental Setup. FBG – Fiber Bragg Grating, WDM – Wavelength Division Multiplexer.

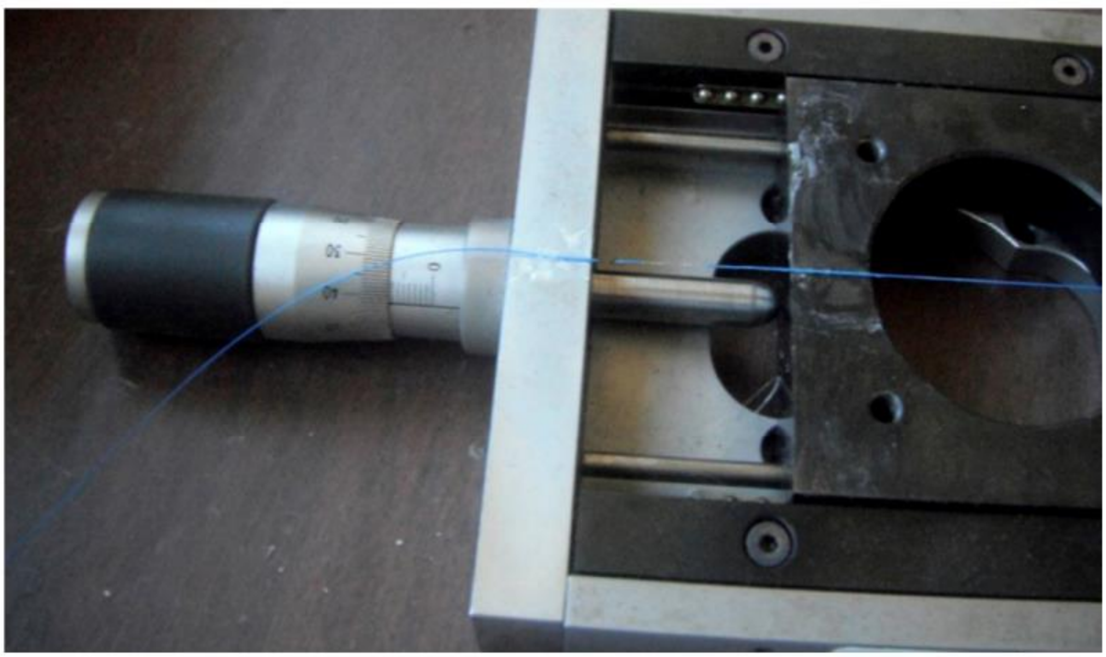

Figure 8: Diagram showing the details of the stretching setup for FBG1.

3.1 Assembling of the Optical Cavity

The optical cavity as used in this experiment was assembled with the use of various techniques and instruments/tool kits. This is indeed important to ensure non-contamination of the optical cavity with impurities such as dust during assembling. The instruments used are splicer and cleavage machine. These are more explained below;

i. Splicer: This machine optimally aligns and join two optical fibers perfectly while estimating the loss in the process. Also called splicing machine, it can help to achieve a very perfect joining of two separate optical fibers when used appropriately. The process majorly involves fusing the two optical fibers together. For this experiment, we used the splicer shown in Figure 9 to join FBG1 to one side of the EDF and FBG2 to the other side of the EDF. Also, the output point of FBG2 was spliced with the input point of the WDM. For all the splicing made in the experiment, we ensured that the loss is minimal and negligible. We obtained the loss estimation of 0.04 *dB*. The four basic steps in fusion splicing are striping of the fiber, cleaving of the fiber using cleavage machine, fusing the fiber and protecting the fiber.

ii. Cleavage machine: The cleavage machine is used to perfectly cut the fiber optical cable after using a dedicated plier to remove the cladding and the core's protection. The cleavage machine is simple to use as it basically involves 1 – 4 steps. These steps are printed on the machine itself. A precaution to take note of is ensuring that the optical fiber is well aligned in the position so as to avoid slanty cut. A prototype of the cleavage machine shown in Figure 10.

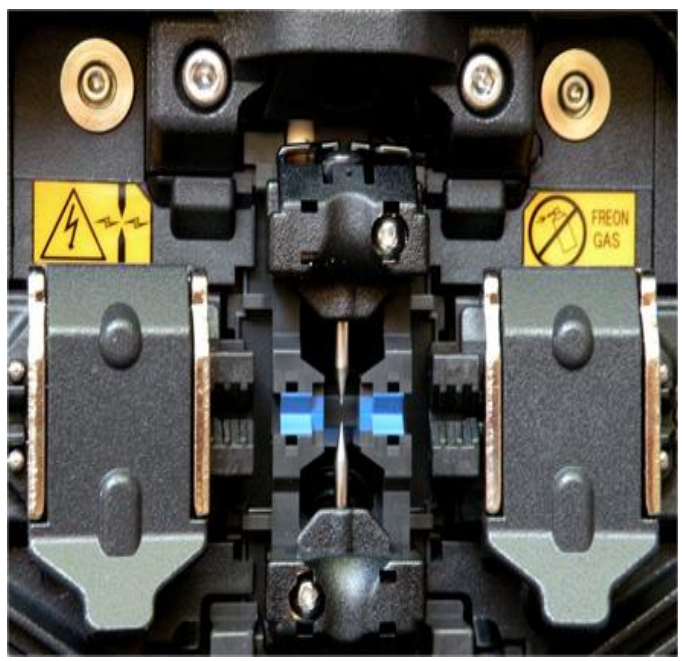

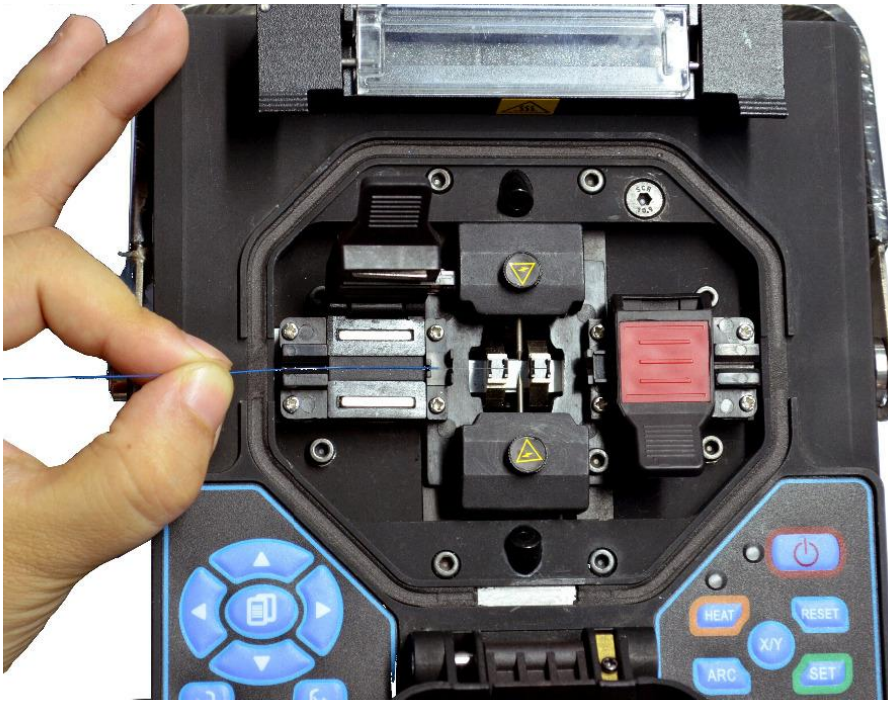

Figure 9: Diagrams showing splicing machine and kits as used in this experiment

Figure 10: Diagrams showing cleaving machine as used in this experiment

4.0 *Results and Discussion*

4.1 *Fiber Bragg Grating Characterization*

We characterized the FBG by measuring the florescence due to the erbium doped fiber with a pump power of 50 *mA*. This was measured when there no strain was applied on the FBG (i.e. when the cavity is detuned) so as to obtain different Bragg peaks for FBG1 and FBG2 respectively. The spectrum was measured using Optical Spectrum Analyzer (OSA) at the near end of the cavity. This spectrum ass recorded in this experiment is shown in figure 11. From figure 11, it is evident from the spectrum the working characteristics of FBG1 and FBG2. The positive peak is of course due to spontaneous emission light being reflected by FBG1 in the far end at its Bragg wavelength while the negative peak is as a result of the reflectivity of FBG2 in the near end.

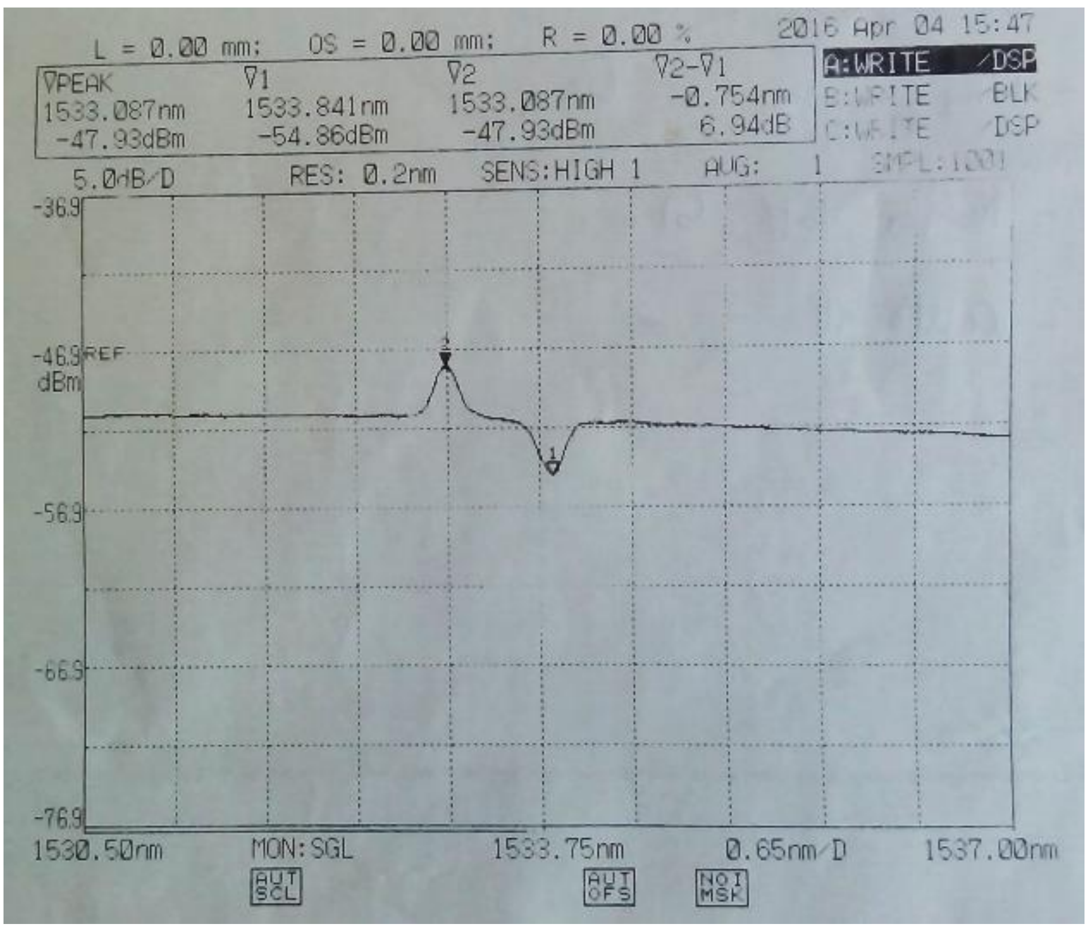

Figure 11: Florescence spectra from the laser showing the effect of the two fiber Bragg gratings without detuning.

Applying strain to FBG1 as discussed earlier affects the position of the Bragg wavelength. This is evident in figure 12 as the peak location is opposite to when the FBG is unstrained. As expected, the positive peak is due to spontaneous emission reflected by FBG1 in the far end and the negative peaks are made by the reflectivity of FBG2 in the near end of the cavity.

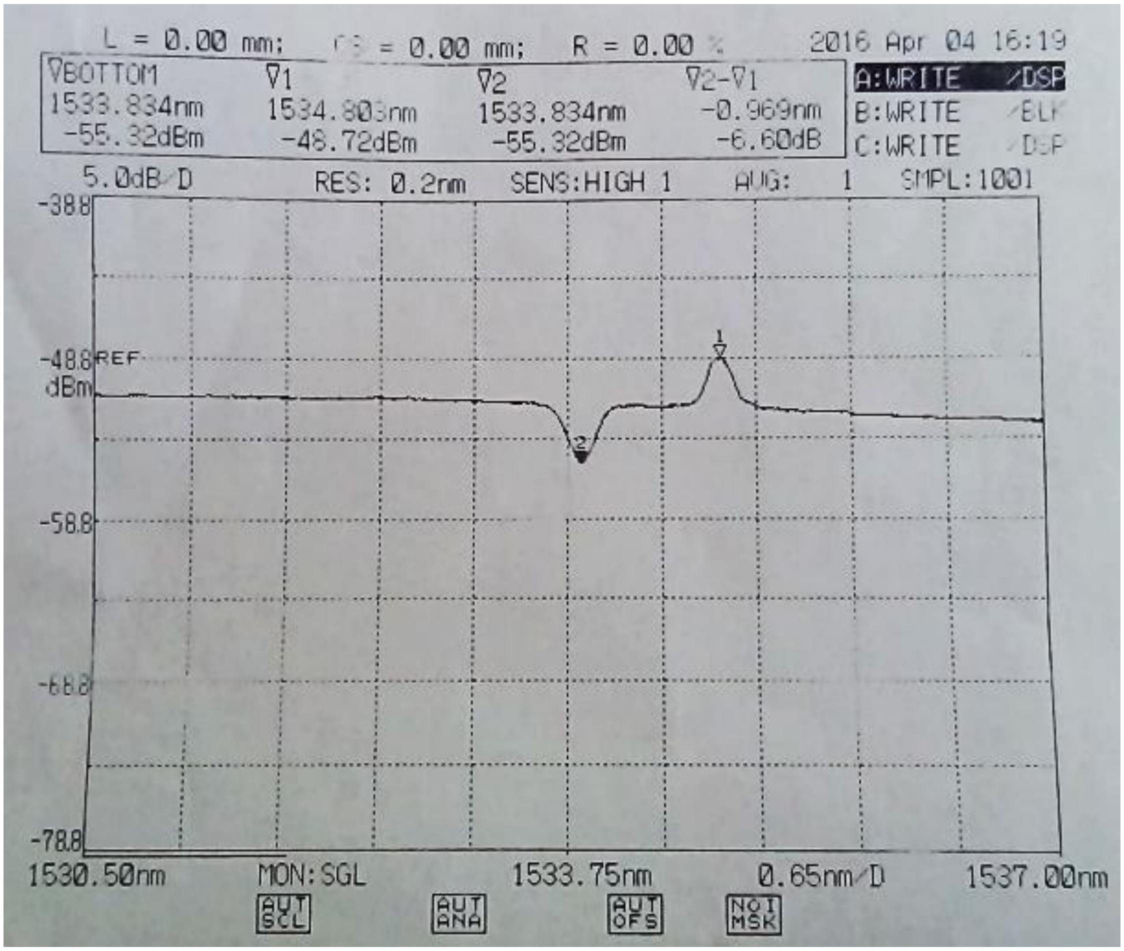

Figure 12: Florescence spectra from the laser showing the effect of the two fiber Bragg gratings when FBG1 is stretched/tuned

4.2 Laser Characterization

4.2.1 Spectral Emission Characteristics

Fiber laser operation should be characterized in terms of laser emission content as a function of the optical pump power increase. For this experiment the FBG1 was stretched until a good overlap with FBG2 is obtained after which the laser spectrum was obtained using the OSA. Figure 13 shows the spectrum obtained for 50 *mA* and 31 *mW* of pump current and power respectively. The spectrum obtained is far above threshold which consequently leads to its deviant characteristics compared to the spectrum in figure 11. The threshold value is 3.0 *dB* and 13.0 *dB* for levels 1 and 2 of the fiber laser. The width of the laser peak was measured to be 0.157 *nm* with a signal to noise ratio of 35 *dB*.

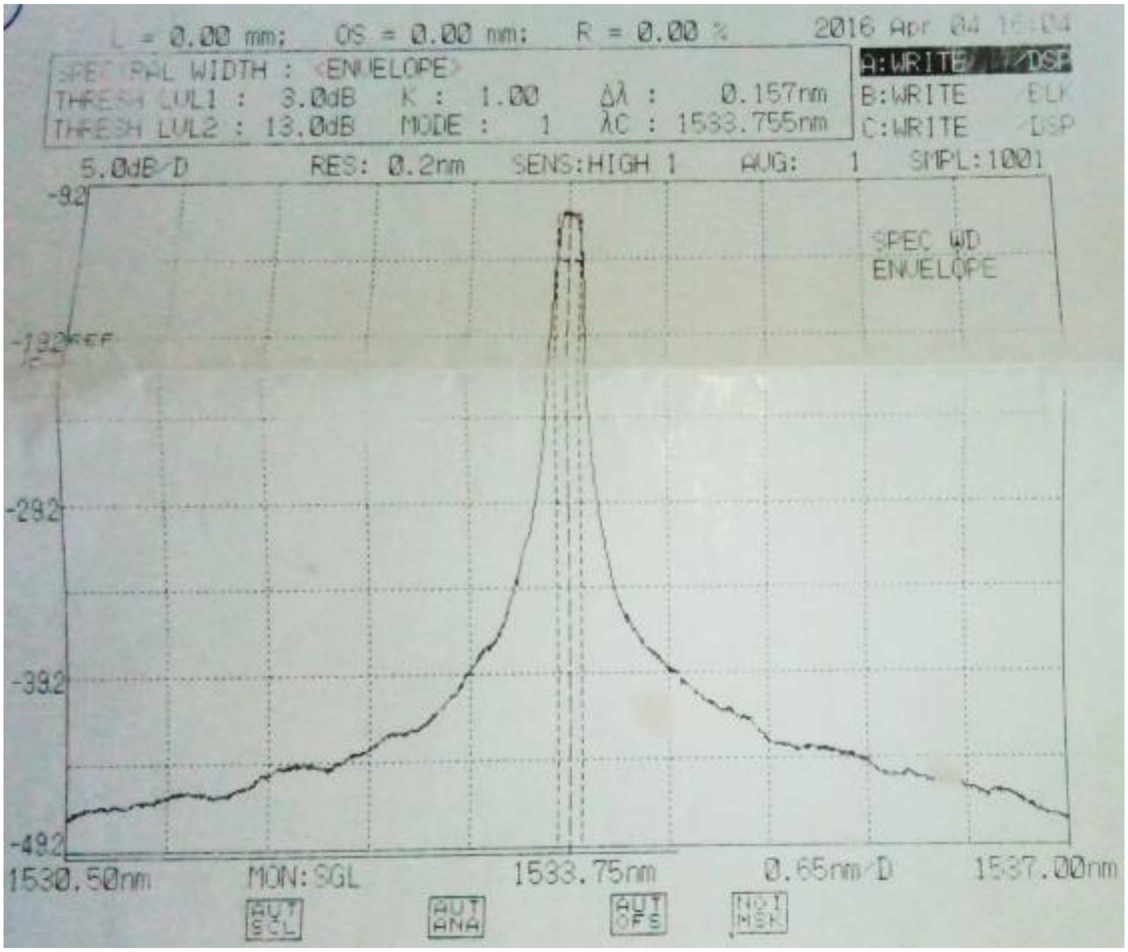

Figure 13: Spectrum emission characteristics of the fiber laser

4.2.2 Laser Power and Laser Threshold Characteristics

In order to study the dependence of laser output power with respect to the pump power, the OSA was replaced with an optical power meter/detector shown in figure 14. Then, measurements of the laser power output were recorded with their respective set of pump power for different stretchings of the FBG1 so as to create different wavelength mismatch. Results obtained for the described setup are presented graphically in Figure 8. For each set of the results of FBG1 stretching, a linear fit was performed along the output power linear behaviour section. This is of course, imperative in order to determine/estimate the threshold pump power value and the slope efficiency of the fiber laser.

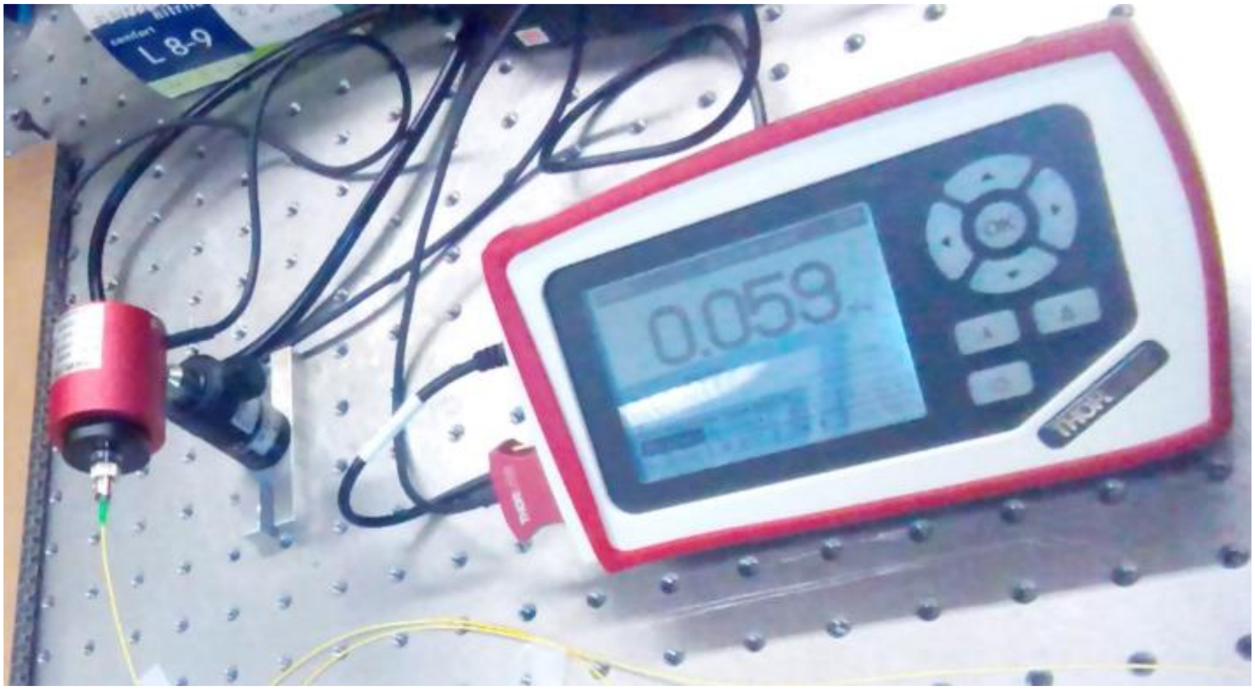

Figure 14: Picture of the optical power meter/detector used in the experiment

In addition, figure 15 reveals the two representative curves which clearly shows that the threshold increases with decreasing reflectivity of the FBGs in the cavity. Also, the best efficiency is not obtained with the lower cavity losses (triangular data point marker) compared to the efficiency obtained with the higher cavity losses (star data point marker). For the low reflectivity, the threshold pump power is estimated to be 0.05176 *mW* with a standard error of 0.01015 while the slope efficiency of the fiber laser is given as 0.00196 *mW/mA* with a standard error of $3{\cdot}832\times10^{-5}$. Also, for high reflectivity, the threshold pump power is estimated to be 0.06258 *mW* with a standard error of 0.03719 while the slope efficiency of the fiber laser is given as 0.00248 *mW/mA* with a standard error of $1{\cdot}244\times10^{-4}$.

5.0 Conclusion

A fiber laser based setup (figure 16) is presented and characterized while aiming at the hands-on study of several photonic devices, namely Fiber Bragg Gratings which were inscribed in fiber and fiber lasers, as well as optical instrumentation and measuring equipments (Splicer, OSA, Optical Power Meter, etc.) allowing the study of some laser features manipulation. Consequently, the experiment allows to visually exploit the major working principle of FBGs during laser cavity tuning/detuning by inducing mechanical stress at one of the FBGs. The laser emission characteristics were then vividly studied by measuring the threshold dependency on the total losses (mirror reflectivity). Also, the determination of an optimal coupler reflectivity was made through the plot of output power against pump power with the detuning. In conclusion, some precautionary measures were taken in the course of the experiment, these are as follows;

i. We ensured the joining of the optical fibers using the splicer and cleaver were carefully made to avoid any contamination from dust.
ii. We ensured careful handling of the optical fibers to avoid any breakage along the propagation path of the cavity.

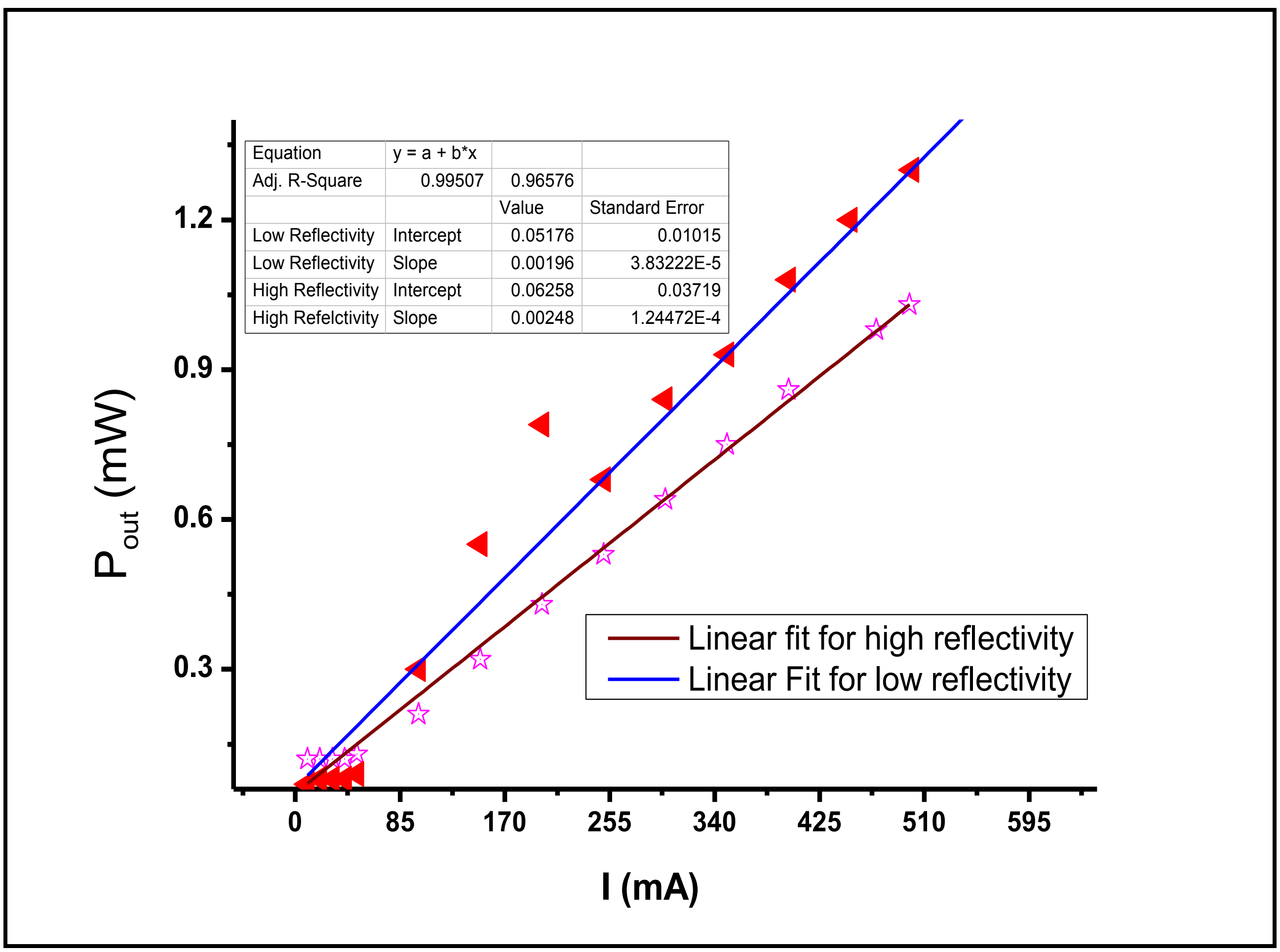

Figure 15: Output power as a function of pump power for different stage positions

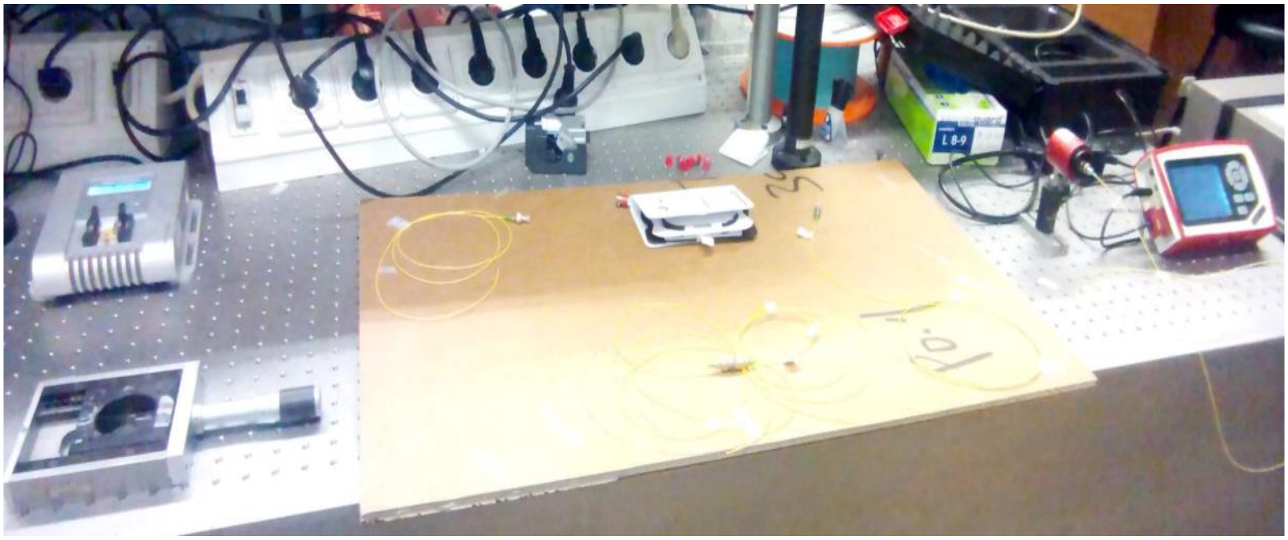

Figure 16: Picture showing the full setup of the fiber laser experiment.

References

1. Agrawal, G. P., Fiber-Optic Communication Systems. third edition, John Wiley and Sons, 2002.
2. Digonnet, M. J. F., editor, Rare-Earth-Doped Fiber Lasers and Amplifiers, Marcel Dekker, 2001.
3. Tünnermann, A., Schreiber, T., and Limpert, J., "Fiber lasers and amplifiers: an ultrafast performance evolution", Applied Optics, 49(25), F71–F78, (2010)
4. Johnstone, W., Culshaw, B., Moodie, D. G., Mauchline I. S., and Walsh, D., "Photonics laboratory teaching experiments for scientists and engineers", Proc. SPIE 4588, Seventh International Conference on Education and Training in Optics and Photonics, 304 (2002).
5. Wen Zhu, W., Qian, and L., Helmy, A. S., "Implementation of three functional devices using Erbium-doped Fibers: An Advanced Photonics Lab", International Conference on Education and Training in Optics and Photonics, ETOP 2007, EXP VIII, (2007).
6. Kashyap, R.; [Fiber Bragg gratings], Academic Press, London, (1999).
7. Othonos, A., "Fiber Bragg gratings", Rev. Sci. Instrum. 68(12), 4309-4342, (1997).
8. Svelto, O., Principles of Lasers, Fifth Edition, Springer, New York, (2010).